

Power law in a microcanonical ensemble with scaling volume fluctuations

V. V. Begun,¹ M. Gaździcki,^{2,3} and M. I. Gorenstein^{1,4}

¹*Bogolyubov Institute for Theoretical Physics, Kiev, Ukraine*

²*Institut für Kernphysik, University of Frankfurt, Frankfurt, Germany*

³*Jan Kochanowski University, Kielce, Poland*

⁴*Frankfurt Institute for Advanced Studies, Frankfurt, Germany*

(Received 18 April 2008; published 15 August 2008)

Volume fluctuations are introduced in a statistical modeling of relativistic particle collisions. The microcanonical ensemble is used, and the volume fluctuations are assumed to have specific scaling properties. This leads to the KNO scaling of the particle multiplicity distributions as measured in $p + p$ interactions. A striking prediction of the model is a power law form of the single particle momentum spectrum at high momenta. Moreover, the mean multiplicity of heavy particles also decreases as a function of the particle mass according to a power law. Finally, it is shown that the dependence of the momentum spectrum on the particle mass and momentum reduces to the dependence on the particle energy. These results resemble the properties of particle production in collisions of high energy particles.

DOI: [10.1103/PhysRevC.78.024904](https://doi.org/10.1103/PhysRevC.78.024904)

PACS number(s): 24.60.-k, 12.40.Ee

I. INTRODUCTION

In collisions at relativistic energies many new particles are produced. Their number, masses, and charges as well as their momenta vary from event to event. Most of the experimental results concern single particle production properties averaged over many interactions. It is well established that some of these properties, namely, mean particle multiplicities and transverse momentum spectra, follow simple rules of statistical mechanics. In proton-proton ($p + p$) collisions the single particle momentum distribution has an approximately Boltzmann form [1] in the local rest frame of produced matter:

$$\frac{dN}{p^2 dp} \sim \exp\left(-\frac{\sqrt{p^2 + m^2}}{T}\right), \quad (1)$$

where T , p , and m are the temperature parameter, the particle momentum and its mass, respectively. At large momentum, $p \gg m$, Eq. (1) gives

$$\frac{dN}{p^2 dp} \sim \exp\left(-\frac{p}{T}\right). \quad (2)$$

Integration of Eq. (1) over momentum yields the mean particle multiplicity, $\langle N \rangle$, which is also governed by the Boltzmann factor for $m \gg T$:

$$\langle N \rangle \sim (mT)^{3/2} \exp\left(-\frac{m}{T}\right). \quad (3)$$

The approximate validity of the exponential distributions (1)–(3) is confirmed by numerous experimental results on bulk particle production in high energy collisions. The agreement is limited to the low transverse momentum ($p_T \leq 2$ GeV) and the low mass ($m \leq 2$ GeV) domains. However, the temperature parameter T extracted from the data on $p + p$ interactions is in the range 160–190 MeV [2]. Thus, almost all particles are produced at low p_T and with low masses. Along with evident successes there are obvious problems of the statistical approach. The probability $P(N)$ to create N particles in $p + p$ collisions obeys the KNO scaling [3] (see also Refs. [4–6]),

namely,

$$P(N) = \langle N \rangle^{-1} \psi(z), \quad (4)$$

where $\langle N \rangle$ is the mean multiplicity and the KNO scaling function $\psi(z)$ only depends on $z \equiv N/\langle N \rangle$. The mean multiplicity increases with increasing collision energy, whereas the KNO scaling function remains unchanged. The latter implies that the scaled variance ω of the multiplicity distribution $P(N)$ grows linearly with the mean multiplicity:

$$\omega \equiv \frac{\langle N^2 \rangle - \langle N \rangle^2}{\langle N \rangle} \propto \langle N \rangle. \quad (5)$$

A qualitatively different behavior is predicted within the existing statistical models [7–9], namely the scaled variance is expected to be independent of the mean multiplicity:

$$\omega \approx \text{const.} \approx 1. \quad (6)$$

This contradiction between the data and the statistical models constitutes the first problem which will be considered in this paper.

The second and the third problems which will be addressed here concern particle production at high (transverse) momenta and with high masses, respectively. In these regions the single particle energy distribution seems to obey a power law behavior [10]:

$$\frac{dN}{p^2 dp} \sim (\sqrt{p^2 + m^2})^{-K}. \quad (7)$$

At $p \gg m$, Eq. (7) gives

$$\frac{dN}{p^2 dp} \sim p^{-K_p}, \quad (8)$$

with $K_p = K$. Integration of Eq. (7) over particle momentum yields the mean multiplicity which follows a power law dependence on the particle mass:

$$\langle N \rangle \sim m^{-K_m}, \quad (9)$$

with $K_m = K_p - 3$. Equations (8) and (9) approximately describe the data on spectra of light particles at large ($p \geq 3$ GeV)

(transverse) momenta and on the mean multiplicity of heavy ($m \geq 3$ GeV) particles, respectively. The power law parameters fitted to the data are $K_p \cong 8$ and $K_m \approx 5$ [10]. One observes a growing disagreement between the exponential behavior (2), (3) and power law dependence (8), (9) with increasing (transverse) momentum and mass. At $p = 10$ GeV or $m = 10$ GeV the statistical models underestimate the data by more than 10 orders of magnitude.

In the present paper we make an attempt to extend the statistical model to the hard domain of high transverse momenta and/or high hadron masses (hard domain). The proposal is inspired by statistical type regularities [10] in the high transverse mass region, as well as by the recent work on the statistical ensembles with fluctuating extensive quantities [11]. We postulate that the volume of the system created in $p + p$ collision changes from event to event.¹ The main assumptions of the proposed approach are the following.

- (i) Each final state created in $p + p$ interactions is identified with a microstate of a microcanonical ensemble (MCE) defined by the volume V , energy E , and conserved charges of the system. By definition of the MCE, all its microstates appear with the same probability.
- (ii) The volume of microcanonical ensembles represented in $p + p$ interactions fluctuates from collision to collision. The volume probability density function, $P_\alpha(V)$, is given by the scaling function, $P_\alpha(V) = \bar{V}^{-1} \phi_\alpha(V/\bar{V})$, where \bar{V} is the scaling parameter.

The model based on these assumptions will be referred as the microcanonical ensemble with scaling volume fluctuations (MCE/sVF). Calculations presented in this work aim to illustrate the main idea and therefore they are performed within the simplest possible model which preserves the essential features: an ideal gas of massless particles and a mixture of massless neutral with heavy neutral particles. The Boltzmann approximation has been used. The paper is organized as follows. The description of the relativistic gas of particles within the MCE is presented in Sec. II. The scaling volume fluctuations within the MCE framework are introduced in Sec. III. Then the basic equations of the MCE/sVF are given. Next, the results on the multiplicity distribution, the single particle momentum spectrum and the mean multiplicity of heavy particles are obtained. The paper ends with the summary and closing remarks presented in Sec. IV.

II. MICROCANONICAL ENSEMBLE

The MCE partition function for the system with N Boltzmann massless neutral particles reads [8,14]

$$W_N(E, V) = \frac{1}{N!} \left(\frac{gV}{2\pi^2} \right)^N \int_0^\infty p_1^2 dp_1 \dots \int_0^\infty p_N^2 dp_N \times \delta \left(E - \sum_{i=1}^N p_i \right) = \frac{1}{E} \frac{A^N}{(3N-1)N!}, \quad (10)$$

¹The volume fluctuations in hadron statistical physics were first introduced in the framework of the isobaric ensemble in Refs. [12,13].

where E and V are the system energy and volume, respectively, g is the degeneracy factor, and $A \equiv gVE^3/\pi^2$. The MCE partition function (10) includes exact energy conservation, but neglects the momentum conservation. The MCE multiplicity distribution is given by

$$P_{\text{mce}}(N; E, V) = \frac{W_N(E, V)}{W(E, V)}. \quad (11)$$

$W(E, V)$ is the total MCE partition function [8]:

$$W(E, V) \equiv \sum_{N=1}^{\infty} W_N(E, V) = \frac{A}{2E} {}_0F_3 \left(; \frac{4}{3}, \frac{5}{3}, 2; \frac{A}{27} \right), \quad (12)$$

where ${}_0F_3$ is the generalized hypergeometric function (see Appendix). For $A \gg 1$ the mean multiplicity equals to [8]

$$\langle N \rangle_{\text{mce}} \equiv \sum_{N=1}^{\infty} N P_{\text{mce}}(N; E, V) \cong (A/27)^{1/4}, \quad (13)$$

where $P_{\text{mce}}(N; E, V)$ was approximated by the normal distribution [8]:

$$P_{\text{mce}}(N; E, V) \cong (2\pi \omega_{\text{mce}} \cdot \langle N \rangle_{\text{mce}})^{-1/2} \times \exp \left[-\frac{(N - \langle N \rangle_{\text{mce}})^2}{2 \omega_{\text{mce}} \cdot \langle N \rangle_{\text{mce}}} \right], \quad (14)$$

with $\omega_{\text{mce}} \equiv (\langle N^2 \rangle_{\text{mce}} - \langle N \rangle_{\text{mce}}^2) / \langle N \rangle_{\text{mce}} = 1/4$. Note that in the grand canonical ensemble (GCE) the multiplicity distribution is equal to the Poisson one:

$$P_{\text{gce}}(N; T, V) = \frac{\bar{N}^N}{N!} \exp(-\bar{N}), \quad (15)$$

where \bar{N} is the mean multiplicity in the GCE. The distribution (15) approaches the Gaussian for large \bar{N} :

$$P_{\text{gce}}(N; T, V) \cong (2\pi \omega_{\text{gce}} \cdot \bar{N})^{-1/2} \exp \left[-\frac{(N - \bar{N})^2}{2 \omega_{\text{gce}} \cdot \bar{N}} \right], \quad (16)$$

with $\omega_{\text{gce}} \equiv (\bar{N}^2 - \bar{N}) / \bar{N} = 1$.

The numerical calculations presented in this paper will be performed for $g = 1$ and the energy density which corresponds to the temperature parameter $T = 160$ MeV. The latter relates the values of E and V via the equation:

$$E = \frac{3}{\pi^2} VT^4. \quad (17)$$

The mean multiplicity $\langle N \rangle_{\text{mce}}$ in the MCE (13) is then approximately equal to the GCE value:

$$\bar{N} = \frac{1}{\pi^2} VT^3. \quad (18)$$

The approximation $\langle N \rangle_{\text{mce}} \cong \bar{N}$ is valid for $\bar{N} \gg 1$ and reflects the thermodynamic equivalence of the MCE and the GCE. The scaled variance of the MCE distribution is $\omega_{\text{mce}} = 1/4$ [8], and is approximately independent of $\langle N \rangle_{\text{mce}}$ already for $\langle N \rangle_{\text{mce}} > 5$. Thus, despite of thermodynamic equivalence of the MCE and GCE the value of ω_{mce} is four times smaller

than the scaled variance of the GCE (Poisson) distribution, $\omega_{\text{gce}} = 1$.

The single particle momentum spectrum in the GCE reads

$$\begin{aligned} F_{\text{gce}}(p) &\equiv \frac{1}{N} \frac{dN}{p^2 dp} = \frac{V}{2\pi^2 N} \exp\left(-\frac{p}{T}\right) \\ &= \frac{1}{2T^3} \exp\left(-\frac{p}{T}\right), \end{aligned} \quad (19)$$

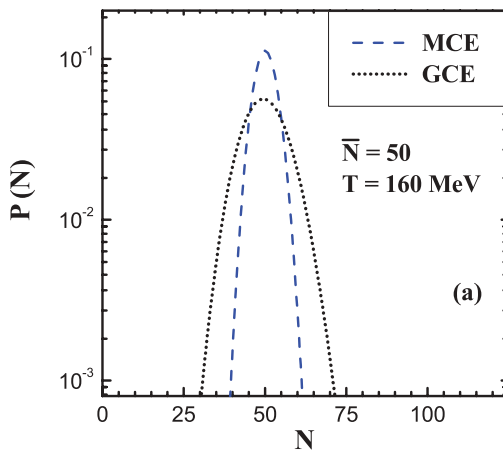
whereas the corresponding spectrum in the MCE is given by

$$\begin{aligned} F_{\text{mce}}(p) &\equiv \frac{1}{\langle N \rangle_{\text{mce}}} \frac{dN}{p^2 dp} = \frac{V}{2\pi^2 \langle N \rangle_{\text{mce}}} \sum_{N=2}^{\infty} \frac{W_{N-1}(E-p, V)}{W(E, V)} \\ &\equiv \frac{V}{2\pi^2 \langle N \rangle_{\text{mce}}} f(p; E, V) \\ &= \frac{1}{\langle N \rangle_{\text{mce}}} \frac{1}{2E^3} \sum_{N=2}^{\infty} \frac{N(3N-1)!}{(3N-4)!} \\ &\quad \times \left(1 - \frac{p}{E}\right)^{3N-4} P_{\text{mce}}(N; E, V), \end{aligned} \quad (20)$$

where $f(p; E, V)$ is the MCE analog of the Boltzmann factor, $\exp(-p/T)$. From Eq. (20) follows $f(p=0; E, V) = 1$. Both Eqs. (19) and (20) are normalized such that $\int_0^{\infty} p^2 dp F_{\text{gce}}(p) = 1$ and $\int_0^E p^2 dp F_{\text{mce}}(p) = 1$.

Figure 1(a) shows a comparison of the MCE and GCE results for the multiplicity distribution and Fig. 1(b) shows the momentum spectrum for $\bar{N} = 50$. The MCE spectrum is close to the Boltzmann distribution (19) at low momenta. This can be shown analytically using the asymptotic form of the generalized hypergeometric function [see Eq. (A4) in Appendix] at $E \rightarrow \infty$ and $p/E \ll 1$:

$$\begin{aligned} f(p; E, V) &= \frac{W(E-p, V)}{W(E, V)} \\ &= \frac{(E-p)^2 {}_0F_3\left(\frac{4}{3}, \frac{5}{3}, 2; \frac{V(E-p)^3}{27\pi^2}\right)}{E^2 {}_0F_3\left(\frac{4}{3}, \frac{5}{3}, 2; \frac{VE^3}{27\pi^2}\right)} \cong \exp\left(-\frac{p}{T}\right). \end{aligned} \quad (21)$$



The MCE spectrum decreases faster than the GCE one at high momenta. Close to the threshold momentum, $p = E$, where the MCE spectrum goes to zero, large deviations from Eq. (19) are observed. In order to demonstrate this the MCE and GCE momentum spectra are shown in Fig. 1(b) over 90 orders of magnitude.

III. MCE WITH SCALING VOLUME FLUCTUATIONS

Let us consider a set of microcanonical ensembles with the same energy E but different volumes V . The probability density which describes the volume fluctuations is denoted by $P_\alpha(V)$. The distribution of any quantity X can then be calculated as

$$P_\alpha(X; E) = \int_0^\infty dV P_\alpha(V) P_{\text{mce}}(X; E, V), \quad (22)$$

where $P_{\text{mce}}(X; E, V)$ is the distribution of the quantity X in the MCE with fixed E and V . Further more it is assumed that the distribution $P_\alpha(V)$ has the scaling form

$$P_\alpha(V) = \bar{V}^{-1} \phi_\alpha(V/\bar{V}), \quad (23)$$

with the volume parameter \bar{V} being the scale parameter of $P_\alpha(V)$. From Eq. (23) follows that the scale parameter is proportional to the average volume and the proportionality factor follows from the normalization conditions of the scaling function (see below). Equations (22) and (23) are the basic equations of the MCE/sVF.

Let us introduce an auxiliary variable y defined as $y \equiv (V/\bar{V})^{1/4}$. Using Eqs. (13) and (17), (18) the mean multiplicity of massless particles in the MCE (13) can be written as

$$\langle N \rangle_{\text{mce}} = \bar{N} y, \quad (24)$$

where

$$\bar{N} = \left(\frac{E^3 \bar{V}}{27\pi^2} \right)^{1/4}. \quad (25)$$

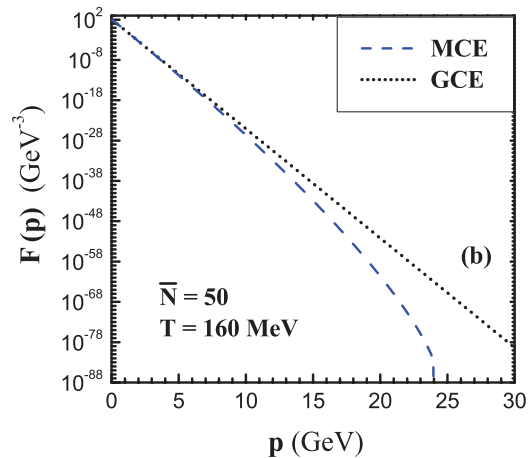


FIG. 1. (Color online) (a) The multiplicity distribution of massless neutral particles in the MCE (11) (dashed line), and the GCE (15) (dotted line). (b) The momentum spectrum of massless neutral particles calculated within the MCE (20) (dashed line) and the GCE (19) (dotted line). The system energy is $E = 3\bar{N}T = 24$ GeV for both plots.

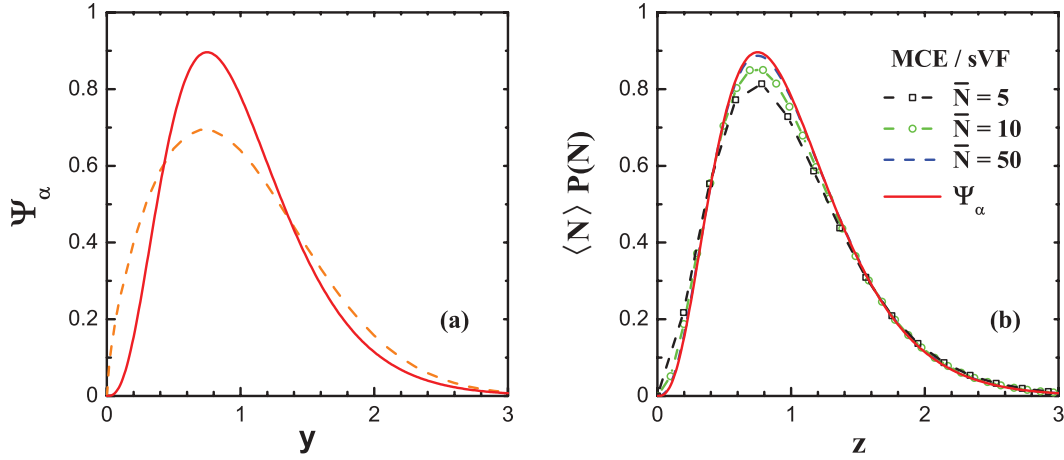


FIG. 2. (Color online) (a) The scaling functions determining the volume fluctuations discussed in this paper. Solid line indicates the function (33) with $k = 4$ for which all presented results are calculated, whereas the dashed line shows the function (34) used for the sensitivity tests. (b) The multiplicity distributions calculated within the MCE/sVF for three values of mean multiplicity. The calculations are performed for the function (33) with $k = 4$. The distributions are presented in the KNO variables, $\langle N \rangle \cdot P(N)$ and $z = N/\langle N \rangle$.

The average temperature \bar{T} is related [see Eq. (17)] to the energy and volume parameter \bar{V} as

$$E = \frac{3}{\pi^2} \bar{V} \bar{T}^4. \quad (26)$$

Within this paper $\bar{T} = 160$ MeV is assumed. The change of the volume at $E = \text{const.}$ leads to the corresponding change of the system temperature:

$$T = \bar{T} \cdot (\bar{V}/V)^{1/4} = \bar{T}/y. \quad (27)$$

The temperature fluctuations resulting from the volume fluctuations will be discussed below.

Using the variable y , the volume integral in Eq. (22) can be conveniently rewritten as

$$\begin{aligned} P_\alpha(X; E) &= (\bar{V})^{-1} \int_0^\infty dV \phi_\alpha(V/\bar{V}) P_{\text{mce}}(X; E, V) \\ &= \int_0^\infty dy \psi_\alpha(y) P_{\text{mce}}(X; E, y^4 \bar{V}), \end{aligned} \quad (28)$$

where $\psi_\alpha(y) \equiv 4y^3 \phi_\alpha(y^4)$. Choosing $\psi_\alpha(y) = \delta(y-1)$ one recovers the MCE with $V = \bar{V}$ and $\langle N \rangle_{\text{mce}} = \bar{N}$.

The scaling function $\psi_\alpha(y)$ will be required to satisfy two normalization conditions:

$$\int_0^\infty dy \psi_\alpha(y) = 1, \quad \int_0^\infty dy y \psi_\alpha(y) = 1. \quad (29)$$

The first condition guarantees the proper normalization of the volume probability density function, $\int_0^\infty dV P_\alpha(V) = 1$. The second condition is selected in order to keep the mean multiplicity in the MCE/sVF equal to the MCE mean multiplicity.

A. KNO scaling

The multiplicity distribution in the MCE/sVF is

$$\begin{aligned} P_\alpha(N; \bar{N}) &= \int_0^\infty dV P_\alpha(V) P_{\text{mce}}(N; E, V) \\ &= \int_0^\infty dy \psi_\alpha(y) P_{\text{mce}}(N; E, y^4 \bar{V}). \end{aligned} \quad (30)$$

At $\bar{N} \gg 1$, the particle number distribution (30) can be approximated as

$$P_\alpha(N; \bar{N}) \cong \langle N \rangle_\alpha^{-1} \psi_\alpha(z), \quad (31)$$

where $z \equiv N/\langle N \rangle_\alpha$, and the mean multiplicity $\langle N \rangle_\alpha$ is given by

$$\langle N \rangle_\alpha = \sum_{N=1}^\infty N P_\alpha(N; \bar{N}) \cong \bar{N} \int_0^\infty dy y \psi_\alpha(y) = \bar{N}. \quad (32)$$

The approximate equality of $\langle N \rangle_\alpha$ and \bar{N} is satisfied for $\bar{N} \gg 1$ due to the second normalization condition (29). The KNO scaling of the multiplicity distribution $P_\alpha(N; \bar{N})$ follows from the assumption of the scaling of the volume fluctuations (23).

For convenience, a simple analytical form of the scaling function, ψ_α will be used:

$$\psi_\alpha(y) = \frac{k^k}{\Gamma(k)} y^{k-1} \exp(-k y), \quad (33)$$

where $\Gamma(k)$ is the Euler gamma function. It was found [13] that the function (33) with $k = 4$ approximately describes the experimental data on KNO scaling in $p + p$ interactions. All numerical calculations obtained within the MCE/sVF and presented in this paper will be done using the function (33) with $k = 4$. Note, that the function (33) satisfies both normalization conditions (29) for any $k > 0$. In order to check the sensitivity of the results derived within the MCE/sVF to the shape of the KNO scaling function, the calculations presented below were repeated using the scaling function resulting from the fit to the experimental data [4]:

$$\psi_\alpha(y) = a y^c \exp(-b y^2), \quad (34)$$

where the values of the parameters are the following: $a = 1.19$, $b = 0.62$, and $c = 0.66$.

In Fig. 2(a) both KNO scaling functions (33) and (34) are plotted for a comparison. The qualitative behavior is similar, however there are substantial quantitative differences.

Nevertheless, the main results presented below are the same for both scaling functions.

The multiplicity distributions calculated within the MCE/sVF for the three mean multiplicities, $\bar{N} = 5, 10,$ and $50,$ are shown in Fig. 2(b) in the KNO variables. The scaling function (33) is also shown for a comparison. These numerical results indicate that even for relatively low mean multiplicities the KNO scaling is approximately obeyed by the MCE/sVF distributions.

The KNO scaling of the multiplicity distribution implies that the scaled variance of the distribution increases in proportion to the mean multiplicity. For $\bar{N} \gg 1$ one gets

$$\omega_\alpha = \frac{\langle N^2 \rangle_\alpha - \langle N \rangle_\alpha^2}{\langle N \rangle_\alpha} \cong \kappa \langle N \rangle_\alpha, \quad (35)$$

where $\kappa = \text{const.} > 0.$ Equation (35) results from an approximation of $\langle N^2 \rangle_\alpha$ for $\bar{N} \gg 1,$ namely,

$$\begin{aligned} \langle N^2 \rangle_\alpha &= \sum_{N=1}^{\infty} N^2 P_\alpha(N; \bar{N}) \cong \bar{N}^2 \int_0^{\infty} dy y^2 \psi_\alpha(y) \\ &\cong (1 + \kappa) \langle N \rangle_\alpha^2. \end{aligned} \quad (36)$$

The positive value of κ in Eq. (36) follows from the normalization conditions (29):

$$\kappa = \int_0^{\infty} dy y^2 \psi_\alpha(y) - 1 = \int_0^{\infty} dy (y - 1)^2 \psi_\alpha(y) > 0. \quad (37)$$

For the function $\psi_\alpha(y)$ defined by Eq. (33) one finds, $\kappa = k^{-1}.$

In Fig. 3 the multiplicity distributions obtained within the MCE and the MCE/sVF for $\bar{N} = 50$ are compared. The scaled variance of the MCE/sVF distribution for $\bar{N} = 50$ is about 12.5, whereas the scaled variance of the MCE distribution is 1/4. This large difference in the width of the MCE/sVF and the MCE distributions is clearly seen in the figure.

The volume averaging procedure results in the mean value given by

$$\langle V \rangle_\alpha = \int_0^{\infty} dV V P_\alpha(V) = \bar{V} \int_0^{\infty} dy y^4 \psi_\alpha(y) \equiv a \bar{V}. \quad (38)$$

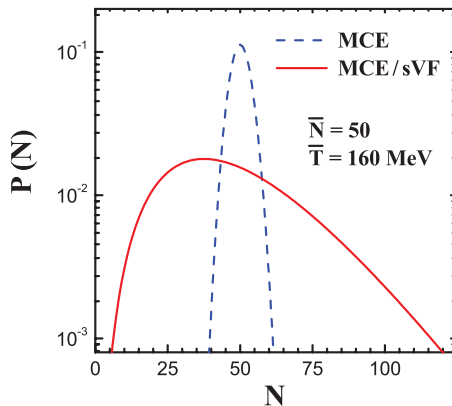


FIG. 3. (Color online) A comparison of the multiplicity distributions of massless neutral particles calculated with the MCE/sVF (solid line) and the MCE (dashed line). The system energy is $E = 3\bar{N}\bar{T} = 24$ GeV.

For ψ_α Eq. (33) one gets

$$a = \frac{(k+1)(k+2)(k+3)}{k^3}, \quad (39)$$

which gives $a \cong 3.28$ for $k = 4.$ Thus, in general, the mean volume in the MCE/sVF is not equal to the corresponding MCE volume.

B. Power law in momentum spectrum

The volume fluctuations in the MCE/sVF significantly increase the width of the multiplicity distribution. They are also expected to modify the single particle momentum spectrum. This is because for a fixed system energy, the volume of the system determines the energy density, and consequently, the effective temperature of particles.

The single particle momentum spectrum within the MCE/sVF can be directly calculated from Eq. (22) and it reads

$$\begin{aligned} F_\alpha(p) &\equiv \frac{1}{\langle N \rangle_\alpha} \left\langle \frac{dN}{p^2 dp} \right\rangle_\alpha \\ &= \frac{1}{\langle N \rangle_\alpha} \int_0^{\infty} dV P_\alpha(V) \frac{V}{2\pi^2} f(p; E, V) \\ &= \frac{1}{\langle N \rangle_\alpha} \frac{1}{2E^3} \sum_{N=2}^{\infty} \frac{N(3N-1)!}{(3N-4)!} \\ &\quad \times \left(1 - \frac{p}{E}\right)^{3N-4} P_\alpha(N; \bar{N}). \end{aligned} \quad (40)$$

The formal structure of the expression (40) is similar to the structure of the corresponding expression derived within the MCE (20). The only, but the crucial, difference is that the narrow MCE multiplicity distribution used for averaging the particle spectrum in Eq. (20) is replaced by the broad MCE/sVF multiplicity distribution in Eq. (40). The spectrum $F_\alpha(p)$ fulfills the normalization condition, $\int_0^E p^2 dp F_\alpha(p) = 1.$ From Eq. (40) one finds $F_\alpha(p=0) = a \cdot F_{\text{gce}}(p=0).$ Equation (39) gives $a \cong 3.28$ for the ψ_α function (33) with $k = 4.$ Thus, in the MCE/sVF there is an enhancement of the momentum spectrum at $p \rightarrow 0$ compared to the GCE and MCE results.

The single particle momentum spectrum calculated with the MCE/sVF for the volume scaling function (33) is shown in Fig. 4(a). A striking new feature of this spectrum is the presence of a long power law tail. In the momentum range from several GeV to about 20 GeV the spectrum can be approximated by

$$F_\alpha(p) \cong C_p p^{-K_p}, \quad (41)$$

with C_p and K_p being the normalization and power parameters, respectively. For momenta smaller than 3 GeV the spectrum starts to deviate significantly from the power law parametrization and its local inverse slope parameter is close to the temperature of the corresponding GCE, $\bar{T} = 160$ MeV. This is shown in Fig. 4(b), where the momentum spectrum for $p \leq 3$ GeV is presented. A rapid decrease of the spectrum starts at $p \geq 20$ GeV, when the threshold value $p = 24$ GeV is approached. The above features of the MCE/sVF momentum spectrum resemble features of the

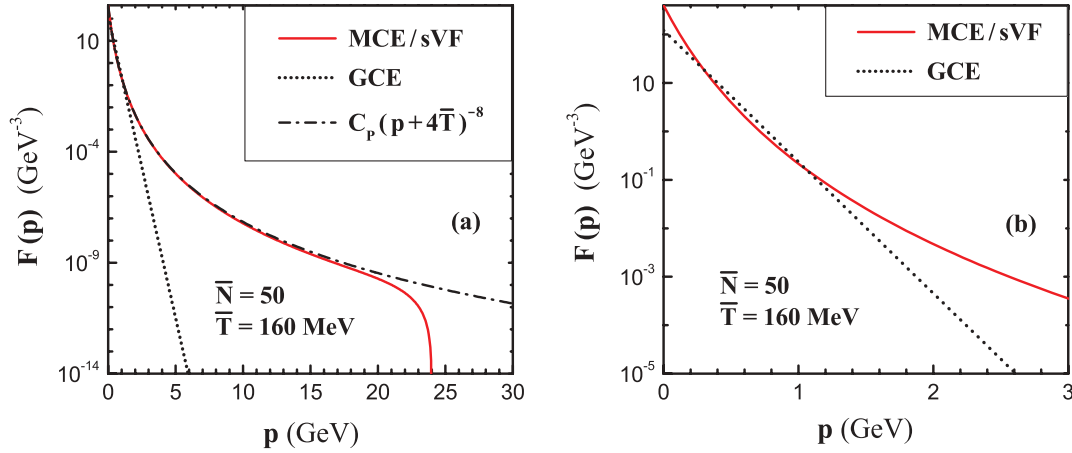


FIG. 4. (Color online) (a) The momentum spectrum of massless neutral particles calculated within the MCE/sVF (40) (solid line), and the GCE (19) (dotted line). The approximation (42) of the MCE/sVF spectrum is shown by the dashed-dotted line. (b) The same as in the left panel but only for the low momentum region. The approximation (42) is not shown as it overlaps with the MCE/sVF line. The system energy is $E = 3\bar{N}\bar{T} = 24$ GeV for both plots.

transverse momentum spectrum of hadrons produced in high energy $p + p$ interactions [15].

The power law dependence (41) of the momentum spectrum at high momenta can be derived analytically, namely,

$$\begin{aligned}
F_\alpha(p) &= \int_0^\infty F_{\text{mce}}(p) \psi_\alpha(y) dy \\
&\cong \frac{\bar{V}}{2\pi^2\bar{N}} \int_0^\infty dy \psi_\alpha(y) y^4 \exp\left(-\frac{p}{\bar{T}} y\right) \\
&= \frac{k^k \Gamma(k+4)}{2\Gamma(k)} \bar{T}^{k+1} (p + \bar{T}k)^{-k-4} \\
&\cong 11.27 \text{ GeV}^5 (p + 4\bar{T})^{-8}, \tag{42}
\end{aligned}$$

where $\bar{T} = 160$ MeV and $k = 4$ is set in the last expression. Note that according to Eq. (27) the temperature, $T = \bar{T}/y$, fluctuates² in the MCE/sVF due to the volume fluctuations. The volume fluctuations are responsible for the appearance of the power law tail. The temperature probability distribution can be easily derived:

$$P(T) = \frac{\bar{T}}{T^2} \psi_\alpha(\bar{T}/T) = \frac{1}{\bar{T}} \frac{k^k}{\Gamma(k)} \left(\frac{\bar{T}}{T}\right)^{k+1} \exp\left(-k \frac{\bar{T}}{T}\right). \tag{43}$$

The result is shown in Fig. 5(b).

The analytical approximation in Eq. (42) is valid for $p \ll E$. It describes the particle spectra at $p \ll E$ including the low momentum region (see Fig. 4(a)). For $p \gg \bar{T}$ one gets the power law parameters (41): $C_p \cong 11.27 \text{ GeV}^{-5}$ and $K_p = 8$. The power law dependence of the particle energy spectrum appears when there is a distinct region of the particle energies in which $\bar{T} \ll p \ll E$.

Equation (42) leads to an exponential spectrum for $p \ll \bar{T}$:

$$F_\alpha(p) \cong \frac{a}{2\bar{T}^3} \exp\left(-\frac{p}{T_0}\right), \tag{44}$$

with the inverse slope parameter $T_0 = \bar{T}/2$ and the normalization constant $a \cong 3.28$. For arbitrary $k > 0$, the parameter a is given by Eq. (39), and $T_0 = \bar{T}k/(k+4)$. Within the used approximation the power parameter, K_p , depends only on the form of the volume scaling function, whereas the normalization constant C_p in Eq. (41) is sensitive, in addition, to the temperature \bar{T} .

Note that the scaling volume fluctuations at a fixed system energy lead alone to the KNO scaling and the power law behavior of the spectra. Systems with small volume, $V \ll \bar{V}$, have predominately a small particle multiplicity, $N \ll \bar{N}$. Due to the energy conservation these systems have large temperatures, $T \gg \bar{T}$, which results in the power law behavior of the momentum spectra and the mean heavy particle multiplicity (see the next section). The energy fluctuations at fixed volume do not lead to the power law dependence. This is because, systems with a small energy, $E \ll \bar{E}$, have predominately a small particle multiplicity, $N \ll \bar{N}$, and consequently the temperature is approximately independent of the system energy, volume or multiplicity. Thus, no power law behavior appears in this case.

On the other hand, the energy fluctuations can be added into the present consideration. They do not change the principal behavior of particle spectra. In order to illustrate the independence of the power law tail of the system energy the MCE/sVF spectra calculated for three different values of E and compared in Fig. 5(a). In the overlapping power law region (left to the cuts from the energy conservation) the spectra are similar, i.e., they do not depend on the average multiplicity. This implies that averaging over collisions with different energies deposited for particle production would not change the particle spectra for momenta below the region affected

²In Ref. [16] it was shown for the first time that the properly chosen temperature fluctuations may lead to the Tsallis distribution [17] with power law spectrum at high (transverse) momenta, see also Ref. [18].

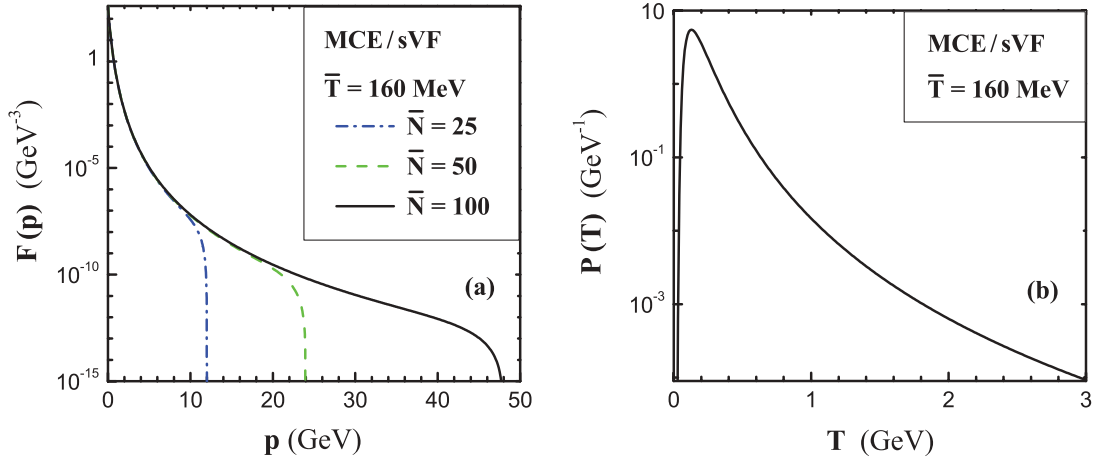


FIG. 5. (Color online) (a) The momentum spectrum of massless neutral particles calculated within the MCE/sVF (40) for three values of the mean multiplicity equal to $\bar{N} = 25$, dashed-dotted line, $\bar{N} = 50$ (dashed line), and $\bar{N} = 100$ (solid line). The system energy is $E = 3\bar{N}\bar{T}$. (b) The temperature probability distribution (43) with $k = 4$ in the MCE/sVF.

by the steep threshold decrease. In particular, it follows from Fig. 5(a) that the energy fluctuations in the region $E = 10$ – 50 GeV do not change the momentum spectra at $p < 10$ GeV. The same arguments are applied to the mean multiplicity of heavy particles discussed in the next section and shown in Fig. 6(b).

Finally, it is important to note, that the momentum spectrum for particles with nonzero mass, m , obeys a power law dependence in the particle energy. This is obvious from Eq. (42), because the particle momentum, p , in the exponent can be replaced by the particle energy, $\sqrt{p^2 + m^2}$, resulting in

$$F_\alpha(p) \cong \frac{\bar{V}}{2\pi^2\bar{N}} \int_0^\infty dy \psi_\alpha(y) y^4 \exp\left(-\frac{\sqrt{p^2 + m^2}}{\bar{T}} y\right) \\ = \frac{k^k \Gamma(k+4)}{2\Gamma(k)} \bar{T}^{k+1} (\sqrt{p^2 + m^2} + \bar{T}k)^{-k-4}. \quad (45)$$

Consequently, the dependence of the momentum spectrum on the particle momentum and mass reduces to the dependence on the particle energy. This energy scaling predicted by the MCE/sVF seems to coincide with the scaling in the transverse mass of the quarkonia spectra measured in $p + \bar{p}$ interactions [10].

C. Power law in mass dependence

The volume fluctuations together with the specific scaling function (33) lead to the power law dependence of the momentum spectrum at high momenta. It may be expected that these volume fluctuations will also cause a similar dependence of mean multiplicity of heavy particles on the particle mass. This subject is discussed below in the approximation of heavy and thus nonrelativistic particles.

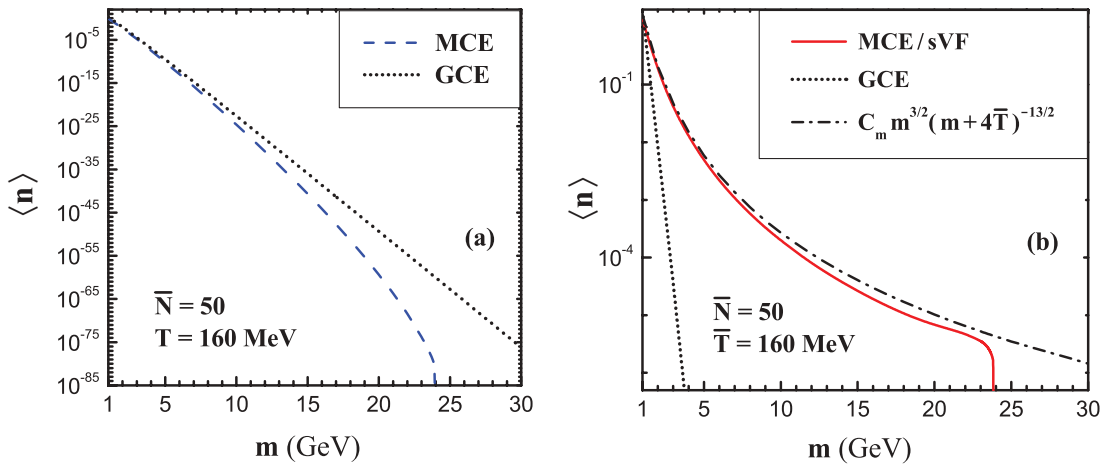


FIG. 6. (Color online) (a) The mean multiplicity of neutral heavy particles, $\langle n \rangle$, as a function of heavy particle mass, m . Note, that the horizontal scale starts at $m = 1$ GeV. The mass dependence obtained with the MCE (48) is indicated by the dashed line, whereas the GCE dependence (49) is shown by the dotted line. The system energy is $E = 3\bar{N}\bar{T} = 24$ GeV. (b) The mass dependence (52) within the MCE/sVF is shown by the solid line, and the dependence for the GCE (49) is indicated by the dotted line. The approximation (54) of the MCE/sVF results is shown by the dashed-dotted line. The system energy is $E = 3\bar{N}\bar{T} = 24$ GeV.

The MCE partition function for n heavy particles is given by [14,19]

$$\begin{aligned}\Omega_n(E, V) &\equiv \frac{1}{n!} \left(\frac{GV}{2\pi^2} \right)^n \int_0^\infty p_1^2 dp_1 \dots \int_0^\infty p_n^2 dp_n \\ &\times \delta \left[E - \sum_{j=1}^n \left(m + \frac{p_j^2}{2m} \right) \right] \\ &= \frac{1}{n!} \left(\frac{GV}{(2\pi)^{3/2}} \right)^n \frac{m^{\frac{3n}{2}}}{\Gamma(\frac{3n}{2})} (E - nm)^{\frac{3n}{2}-1},\end{aligned}\quad (46)$$

where m is the mass of the heavy particle and G is its degeneracy factor. Using Eqs. (10) and (46) one can calculate the MCE partition function for N massless and n heavy particles. It reads [14,19]

$$\begin{aligned}Z_{N,n}(E, V) &= \int_0^\infty dE_1 \int_0^\infty dE_2 W_N(E_1, V) \\ &\times \Omega_n(E_2, V) \delta[E - E_1 - E_2] \\ &= \frac{1}{N!} \frac{1}{n!} \left(\frac{gV}{\pi^2} \right)^N \left(\frac{GV}{(2\pi)^{3/2}} \right)^n \frac{m^{\frac{3n}{2}}}{\Gamma(3N + \frac{3}{2}n)} \\ &\times (E - nm)^{3N + \frac{3n}{2} - 1}.\end{aligned}\quad (47)$$

In what follows the values of the degeneracy factors are assumed to be $g = G = 1$. Note, that due to the exact energy conservation, the MCE partition functions, $W_N(E, V)$ Eq. (10) and $\Omega_n(E, V)$ Eq. (46), are defined for a particle number larger than zero, $N \geq 1$ and $n \geq 1$. However, the MCE partition function, $Z_{N,n}(E, V)$ Eq. (47), requires only $N + n \geq 1$, so that either N or n can be equal to zero. The mean heavy particle multiplicity in the system with two types of particles, massless and heavy, is

$$\langle n \rangle_{\text{mce}} = \frac{1}{Z(E, V)} \sum_{N,n=0}^{\infty} n Z_{N,n}(E, V),\quad (48)$$

where $Z_{N,n}(E, V)$ is given by Eq. (47), $Z(E, V) \equiv \sum_{N,n} Z_{N,n}(E, V)$, and $Z_{0,0}(E, V) = 0$. The energy conservation implies that there is a maximum number of heavy particles, $n_{\text{max}} = \lfloor \frac{E}{m} \rfloor$. Figure 6(a) shows the dependence of the mean multiplicity of heavy particles on mass m calculated within the MCE (48). The plot starts at $m = 1$ GeV. This is because at lower masses, $m \cong T = 160$ MeV, and thus the nonrelativistic approximation used for heavy particles is not justified. Furthermore, if $m \leq 1$ GeV, a contribution of heavy particles to the system energy density can not be neglected, and this would change the temperature parameter T [19]. An exponential decrease with the inverse slope parameter of about 160 MeV observed for masses of several GeV, is followed by a steepening decrease toward the threshold.

At low masses, $m \ll E$, the MCE mean multiplicity is close to the corresponding multiplicity calculated within the GCE, see Fig. 6(a):

$$\bar{n} = V(mT/2\pi)^{3/2} \exp\left(-\frac{m}{T}\right).\quad (49)$$

This can be shown analytically as follows. For the considered values of the total energy E and volume V the average

multiplicity $\langle n \rangle_{\text{mce}}$ is essentially smaller than one. Thus, the main contribution to the numerator of Eq. (48) comes from $Z_{N,n=1}$, while the main contribution to the denominator comes from $Z_{N,n=0}$, thus

$$\begin{aligned}\langle n \rangle_{\text{mce}} &\cong \frac{\sum_{N=0}^{\infty} Z_{N,1}}{\sum_{N=1}^{\infty} Z_{N,0}} \\ &= \frac{\sqrt{2} m^{3/2} \sqrt{E-m}}{E^2} \frac{{}_0F_3\left(\frac{1}{2}, \frac{5}{6}, \frac{7}{6}, \frac{V(E-m)^3}{27\pi^2}\right)}{{}_0F_3\left(\frac{4}{3}, \frac{5}{3}, 2, \frac{VE^3}{27\pi^2}\right)}.\end{aligned}\quad (50)$$

Using Eq. (A4) from the Appendix one can show that in the region $T \ll m \ll E$ it follows:

$$\langle n \rangle_{\text{mce}} \cong \bar{n}.\quad (51)$$

Note that Eq. (50) is valid not only for $\langle n \rangle_{\text{mce}} \ll 1$, but for all values of $\langle n \rangle_{\text{mce}}$ including also $\langle n \rangle_{\text{mce}} \gg 1$. In the limit $VE^3 \rightarrow \infty$ the distribution of heavy particles in the MCE has the Poisson form $P_{\text{mce}}(n) \cong \exp(-\bar{n}) \bar{n}^n / (n!)$, for $nm \ll E$. Thus, $\langle n \rangle_{\text{mce}} \cong P_{\text{mce}}(1) / P_{\text{mce}}(0) \cong \bar{n}$ at all $\bar{n} \ll E/m$.

The mean multiplicity of heavy particles within the MCE/sVF is given by

$$\langle n \rangle_\alpha = \int_0^\infty dy \psi_\alpha(y) \langle n \rangle_{\text{mce}},\quad (52)$$

and its dependence on the mass m is shown in Fig. 6(b). This dependence resembles the behavior of the MCE/sVF momentum spectrum for massless particles shown in Fig. 4.

The mean multiplicity $\langle n \rangle_\alpha$ as a function of m obeys the power law behavior:

$$\langle n \rangle_\alpha \cong \bar{N} C_m m^{-K_m},\quad (53)$$

in the large central interval of heavy particle masses. At high m , the $\langle n \rangle_\alpha$ is larger than corresponding MCE and GCE values by many orders of magnitude. This shows nonequivalence of the MCE/sVF and the GCE or the MCE for mean multiplicity of heavy particles even in the thermodynamic limit. Another example of such nonequivalence was already obtained for the mean volume, see Eq. (38). For the masses close to the threshold mass, $m = 24$ GeV, the mean multiplicity steeply decreases to zero. The power law approximation of the mass dependence can be derived analytically:

$$\begin{aligned}\langle n \rangle_\alpha &= \int_0^\infty dy \psi_\alpha(y) \langle n \rangle_{\text{mce}} \\ &\cong \left(\frac{m\bar{T}}{2\pi} \right)^{3/2} \bar{V} \int_0^\infty dy \psi_\alpha(y) y^{5/2} \exp\left(-\frac{my}{\bar{T}}\right) \\ &= \bar{N} \frac{\sqrt{\pi} k^k \Gamma(k+5/2)}{2\sqrt{2}\Gamma(k)} \frac{\bar{T}^{k+1} m^{3/2}}{(m+\bar{T}k)^{k+5/2}} \\ &\cong \bar{N} \cdot 0.81 \cdot \text{GeV}^5 \frac{m^{3/2}}{(m+\bar{T}k)^{13/2}}.\end{aligned}\quad (54)$$

In the last expression $\bar{T} = 160$ MeV and $k = 4$ are set. The approximation in Eq. (54) is valid for the particle masses much smaller than the system energy, $m \ll E$. The analytical expression (54) describes the numerical results on particle multiplicity at $1 \text{ GeV} < m \ll E$. This is illustrated in Fig. 6(b), where both are compared. If $m \gg \bar{T}$, the power law

dependence (53) of the mean multiplicity on m appears with $C_m \cong 0.81 \text{ GeV}^5$ and $K_m = 5$. This approximation is valid when there is a distinct region of m in which $\bar{T} \ll m \ll E$.

The relation $K_m = K_p - 3$, suggested by the experimental data and derived using a simple statistical considerations [10], is valid within the MCE/sVF. Note, that also the values of the power law parameters, $K_p = 8$ and $K_m = 5$, are close to the corresponding parameters extracted from the experimental data [10]. Within the MCE/sVF these parameters are, however, dependent on the choice of the volume scaling function. For the function (34) one gets $K_p \cong 5.7$ and $K_m \cong 2.5$. Thus, a quantitative comparison with the data requires further studies.

IV. SUMMARY AND CLOSING REMARKS

In this paper the statistical approach to particle production in high energy collisions is extended. A model called the microcanonical ensemble with scaling volume fluctuations, or the MCE/sVF, is proposed which incorporates volume fluctuations in the microcanonical ensemble. A class of scaling volume fluctuations is considered. Analytical and numerical calculations are performed within the simplest formulation of the model which preserves its qualitative features.

First, it is shown that the model leads to KNO scaling of the multiplicity distribution. The volume scaling function is selected in order to reproduce the KNO scaling function measured in $p + p$ interactions.

Second, the single particle momentum spectrum is calculated for massless particles. The MCE/sVF spectrum has features which resemble properties of the transverse momentum spectrum of hadrons produced in very high energy collisions. In particular, a long power law tail appears as a result of the volume fluctuations.

Third, the dependence of the mean multiplicity of heavy particles on the particle mass is obtained. The mass dependence approximately obeys a power law decrease, similar to what is observed experimentally. The power parameters for the momentum spectrum and the mass dependence of mean multiplicity are related as $K_m \cong K_p - 3$, again, similar to experimental data.

Fourth, it is also shown that for particles with arbitrary mass the dependence of the momentum spectrum on the particle mass and momentum reduces to the dependence on the particle energy.

A quantitative comparison with the experimental data requires a significant additional work, in particular the introduction of the proper degrees of freedom and all related conservation laws.

For more than 30 years the production of hadrons at high transverse momenta and/or with high masses, which follows the power law dependence, is discussed within dynamical QCD based models of parton scattering with a large momentum transfer. In particular, the perturbative QCD calculations quantitatively describe many experimental results. Thus, in view of the evident success of the QCD, the applicability range of the MCE/sVF and a relation of the model to the QCD based approaches should be critically studied.

Clearly, further tests of the MCE/sVF are needed. Other qualitative features of $p + p$ interactions should be discussed. The most important is the jet-like correlations of high transverse momentum particles. These correlations are usually described within the perturbative QCD for hard parton scattering accompanied with phenomenological parton-hadron fragmentation function. It is not yet clear whether the jet structure of particle production at high transverse momenta can be reproduced within the MCE/sVF. Clearly this would require an introduction of the momentum conservation. The multiplicity distributions in $p + p$ collisions obey some additional regularities, e.g., the Golokhvastov scaling of the semi-inclusive spectra [20]. They should be also studied within the MCE/sVF.

An effort to extend the model to nucleus-nucleus collisions is needed. First predictions can, however, be obtained from Eqs. (42) and (54). Namely, the particle momentum distribution at high (transverse) momenta and the mean multiplicity of heavy particles are expected to behave as

$$\frac{dN}{p^2 dp} \cong C_p \langle N \rangle p^{-K_p}, \quad (55)$$

$$\langle n \rangle \cong C_m \langle N \rangle m^{-K_m}, \quad (56)$$

where parameters K_p and K_m in Eqs. (55), (56) depend only on the form of the volume scaling fluctuations, and the parameters C_p and C_m depend, in addition, on the mean temperature. Under the assumption that the volume scaling function and mean temperature are energy and system size independent, the MCE/sVF predicts the proportionality of $dN/(p^2 dp)$ at large p and of $\langle n \rangle$ at large m to the average total multiplicity, $\langle N \rangle$. Data on system size dependence of the mean multiplicity of J/ψ mesons as well as the particle yield at high transverse momenta seem to confirm this prediction [21,22].

ACKNOWLEDGMENTS

We would like to thank F. Becattini, A. S. Golokhvastov, W. Greiner, M. Hauer, I. N. Mishustin, St. Mrowczynski, and P. Seyboth for numerous discussions. This work was in part supported by the Program of Fundamental Researches of the Department of Physics and Astronomy of NAS, Ukraine and the Institute VI - 146 of Helmholtz Gemeinschaft, Germany. V.V.B. would like also to thank for the support of The International Association for the Promotion of Cooperation with Scientists from the New Independent states of the Former Soviet Union (INTAS), Ref. No. 06-1000014-6454.

APPENDIX

The generalized hypergeometric function, also known as the Barnes extended hypergeometric functions defined by the following series [23]:

$${}_pF_q(a_1, a_2, \dots, a_p; b_1, b_2, \dots, b_q; z) = \sum_{k=0}^{\infty} \frac{(a_1)_k (a_2)_k \dots (a_p)_k z^k}{(b_1)_k (b_2)_k \dots (b_q)_k k!}, \quad (A1)$$

where $(a)_k$ is the Pochhammer symbol:

$$(a)_k \equiv \frac{\Gamma(a+k)}{\Gamma(a)} = a(a+1)\cdots(a+k-1). \quad (\text{A2})$$

The Euler gamma function $\Gamma(x)$ has a simple form for integer k and half-integer $k + 1/2$ arguments:

$$\Gamma(k) = (k-1)!, \quad \Gamma\left(k + \frac{1}{2}\right) = \frac{1 \cdot 3 \cdot \dots \cdot (2k-1)}{2^n} \sqrt{\pi}. \quad (\text{A3})$$

The asymptotic behavior at $z \rightarrow \infty$ of the hypergeometric function ${}_pF_q$ for $p = 0$ and $q = 3$ is given by [23]

$$\begin{aligned} & {}_0F_3(; b_1, b_2, b_3; z) \\ & \simeq \frac{\Gamma(b_1)\Gamma(b_2)\Gamma(b_3)}{4\sqrt{2}\pi^{3/2}} \exp[4\sqrt[4]{z}] \cdot z^{\frac{1}{4}(\frac{3}{2}-b_1-b_2-b_3)} \\ & \times \left(1 + O\left(\frac{1}{\sqrt[4]{z}}\right)\right). \end{aligned} \quad (\text{A4})$$

-
- [1] R. Hagedorn, *Nuovo Cimento Suppl.* **3**, 147 (1965).
 [2] F. Becattini and U. Heinz, *Z. Phys. C* **76**, 269 (1997); F. Becattini, L. Bellucci, and G. Passaleva, *Nucl. Phys. B, Proc. Suppl.* **92**, 137 (2001).
 [3] Z. Koba, H. B. Nielsen, and P. Olesen, *Nucl. Phys.* **B40**, 317 (1972).
 [4] P. Slattery, *Phys. Rev. Lett.* **29**, 1624 (1972); *Phys. Rev. D* **7**, 2073 (1973).
 [5] M. Gazdzicki, R. Szwed, G. Wrochna, and A. K. Wroblewski, *Mod. Phys. Lett. A* **6**, 981 (1991).
 [6] A. I. Golokhavastov, *Yad. Fiz.* **64**, 88 (2001); **64**, 1924 (2001).
 [7] V. V. Begun, M. Gazdzicki, M. I. Gorenstein, and O. S. Zozulya, *Phys. Rev. C* **70**, 034901 (2004).
 [8] V. V. Begun, M. I. Gorenstein, A. P. Kostyuk, and O. S. Zozulya, *Phys. Rev. C* **71**, 054904 (2005).
 [9] V. V. Begun, M. I. Gorenstein, M. Hauer, V. P. Konchakovski, and O. S. Zozulya, *Phys. Rev. C* **74**, 044903 (2006); V. V. Begun, M. Gazdzicki, M. I. Gorenstein, M. Hauer, V. P. Konchakovski, and B. Lungwitz, *ibid.* **76**, 024902 (2007); M. Hauer, V. V. Begun, and M. I. Gorenstein, arXiv:0706.3290 [nucl-th].
 [10] M. Gazdzicki and M. I. Gorenstein, *Phys. Lett.* **B517**, 250 (2001).
 [11] M. I. Gorenstein and M. Hauer, arXiv:0801.4219 [nucl-th].
 [12] M. I. Gorenstein, *Sov. J. Nucl. Phys.* **31**, 845 (1980) [*Yad. Fiz.* **31**, 1630 (1980)].
 [13] S. Mrowczynski, *Z. Phys. C* **27**, 131 (1985).
 [14] E. Fermi, *Prog. Theor. Phys.* **5**, 570 (1950).
 [15] E. W. Beier *et al.*, *Phys. Rev. D* **18**, 2235 (1978).
 [16] G. Wilk and Z. Włodarczyk, *Phys. Rev. Lett.* **84**, 2770 (2000).
 [17] C. Tsallis, *J. Stat. Phys.* **52**, 479 (1988).
 [18] G. Wilk and Z. Włodarczyk, *Physica A* **376**, 279 (2007).
 [19] V. V. Begun, L. Ferroni, M. I. Gorenstein, M. Gazdzicki, and F. Becattini, *J. Phys. G* **32**, 1003 (2006).
 [20] A. I. Golokhavastov, *Phys. At. Nucl.* **67**, 337 (2004) [*Yad. Fiz.* **67**, 355 (2004)].
 [21] M. Gazdzicki and M. I. Gorenstein, *Phys. Rev. Lett.* **83**, 4009 (1999).
 [22] B. B. Back *et al.* (PHOBOS Collaboration), *Phys. Lett.* **B578**, 297 (2004).
 [23] Eric W. Weisstein, “Generalized Hypergeometric Function,” from *Math World—A Wolfram Web Resource*, <http://mathworld.wolfram.com/Generalized-Hypergeometric-Function.html>, <http://functions.wolfram.com/Hypergeometric-Functions/Hypergeometric-PFQ/06/02/05/>.